

Role of π-Electron Systems in Stabilization of the Oxidized Tetraheme Architecture in Cytochrome c_3

Yuki Takayama,[1,2,†] Midori Taketa-Sato,[3] Hirofumi Komori,[3,4] Kumiko Morita,[3] Su-Jin Kang,[5] Yoshiki Higuchi,[3,4] and Hideo Akutsu*[1,5]

[1]Institute for Protein Research, Osaka University, Yamadaoka, Suita, Osaka 565-0871

[2]Institute for Bioinformatics and Development, Japan Science and Technology Agency, Chiyoda-ku, Tokyo 102-8666

[3]Graduate School of Life Science, University of Hyogo, Koto, Kamigori, Akou-gun, Hyogo 678-1297

[4]The RIKEN SPring-8 Center, Koto, Sayo-cho, Sayo-gun, Hyogo 679-5248

[5]Department of Biophysics and Chemical Biology, Seoul National University, Kwanak-gu, Seoul, Korea

Received February 7, 2011; E-mail: akutsu@protein.osaka-u.ac.jp

Cytochrome c_3 possesses four hemes in a compact configuration and exhibits extremely low reduction potentials. Besides the well-characterized factors contributing to the reduction potentials, the aromatic rings have been suggested to be involved. To elucidate its mechanism, the effect of mutations at conserved and noncoordinated aromatic residues on the reduction/oxidation properties of heme irons was investigated on the basis of crystal structures, NMR spectra of coordinated His, and reduction potentials. Phe20 parallel to heme 1 is the most conserved residue. On its mutation, the change in each coordination structure was subtle in the crystal structures despite of significant changes in the NMR spectra and reduction potentials. Significant increases in the reduction potentials of heme 1 led to the conclusion that the aromatic ring of Phe20 stabilizes the polarization of the π-electron density induced by the oxidized iron in the same heme. Furthermore, the reduction potential of heme 2 was also affected by the mutation at Phe20, revealing that the electrostatic interaction between the π-electron system of the porphyrin and a distant iron contributes to the iron reduction potential. This kind of interaction provides new insight into the role of the heme architecture in regulation of the reduction potentials.

Cytochrome c_3 (cyt c_3) isolated from sulfate-reducing bacteria possesses four *c*-type hemes in a quadrilateral (or cyclic) configuration in a single polypeptide, whose molecular weight is typically ≈14 kDa. The three-dimensional structures of ferric and ferrous cyts c_3 from various strains have been determined by X-ray crystallography and nuclear magnetic resonance (NMR) spectroscopy.[1,2] The important property of cyt c_3 is its extremely low reduction potentials, ranging from −90 to −380 mV.[2] This means that the four positive irons in the hydrophobic core are extensively stabilized in the fully oxidized cyt c_3. We have carried out a series of investigations to clarify the mechanism underlying this stabilization, namely, the extremely low reduction potentials of *Desulfovibrio vulgaris* Miyazaki F (*Dv*MF) cyt c_3 (Figure 1). In these investigations, we have clarified the major factors contributing to the extremely low reduction potentials of *Dv*MF cyt c_3 in comparison with a mitochondrial cyt *c* (about 560 mV higher than the midpoint potential of cyt c_3). The bishistidine coordination decreases the reduction potentials by more than 220 mV with respect to the Met/His coordination.[4] Hydrogen bonding with an axial ligand and an apparent π–π interaction between the aromatic ring and the axial imidazole decrease the reduction potential of a particular heme by 30–50 mV, respectively.[5–7] In addition, the higher heme exposure in cyt c_3 (about 17%) is a well-known contribution.[4] With simple estimation[8] one can expect a

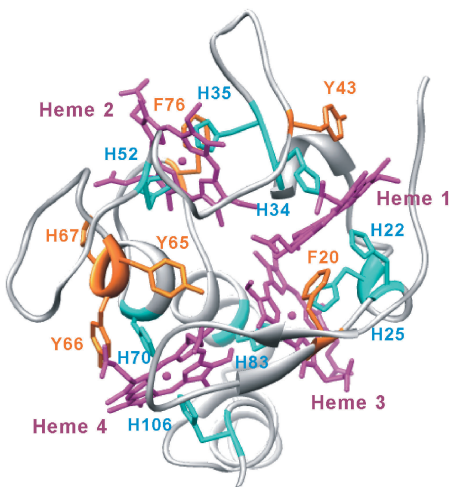

Figure 1. The crystal structure of the oxidized cytochrome c_3 from *Desulfovibrio vulgaris* Miyazaki F (PDB ID, 1J0O). Hemes, coordinated histidines, and noncoordinated aromatic residues are color-coded magenta, cyan, and yellow, respectively. Amino acid residues are denoted by one-letter codes. The figure was prepared with UCSF Chimera.[3]

† Present address: Laboratory of Chemical Physics, National Institute of Diabetes, Digestive and Kidney Disease, National Institutes of Health, Bethesda, MD 20892, USA

Published on the web October 15, 2011; doi:10.1246/bcsj.20110039

≈180 mV decrease in comparison with the reduction potential of a mitochondrial cyt *c* (4% exposure). These contributions account for about 480 out of 560 mV. The quadrilateral tetraheme-architecture of cyt c_3 could be an additional factor, since the midpoint potential for a chain tetraheme-architecture (small tetraheme cyt *c*) increases by more than 100 mV in comparison with that for the quadrilateral tetraheme-architecture of cyt c_3.[9] However, the nature of the interaction in the tetraheme-architecture is not yet clear.

In these investigations, we mutated all aromatic amino acid residues one by one[2,4–7] because the first mutation at Tyr43 suggested a certain contribution of the aromatic ring to lowering of the reduction potentials.[5] There are 14 aromatic residues and four heme rings as π-electron systems in a 107-residue protein. It turned out that only conserved residues, i.e., Phe20, Tyr43, Tyr65, Tyr66, and all coordinated His residues, contributed to the extremely low reduction potentials to some extent, respectively. Phe20, Tyr43, and Tyr66 were proposed to be involved in the apparent π–π interaction with axial imidazoles, respectively. Furthermore, the mutations at Phe20, and Tyr65 affected the reduction potentials of not only the local heme but also distant ones. Phe20 is known as the most conserved residues in all cytochromes c_3, taking a unique structure, in which its aromatic ring is stacked with the porphyrin of heme 1 and the axial imidazole (His25) of heme 3. However, the role of Phe20 in the regulation of the reduction potential is not yet clear as well.

A possible mechanism underlying the effect of mutation on the distant hemes is the propagation of the conformational change from the mutated site to the coordination structure of interest. Therefore, we decided to determine the coordination structures of the mutated proteins in detail with X-ray crystallography and characterize the NMR signals of the coordinated His C2 protons. The obtained results revealed that Phe20 stabilizes the polarization of the π-electron density of the porphyrin induced by the oxidized iron in heme 1 through the π–π interaction. The π-electron system of heme 1 is also involved in the electrostatic interaction with the oxidized iron of heme 2, a distant heme.

Experimental

Preparation of Mutated Proteins. All the mutants used in this study were reported previously.[6] Mutated *Dv*MF cyts c_3 were expressed in *Shewanella oneidensis* and purified according to a reported method.[10]

NMR Measurements. Cyts c_3 were dissolved in 30 mM deuterated sodium phosphate buffer, p^{2}H 7.0. The protein concentrations were ≈1 mM. One-dimensional NMR spectra at 500 MHz were recorded at 303 K with an AVANCE DRX-500 NMR spectrometer (Bruker Biospin, Karlsruhe, Germany). Chemical shifts are presented in parts per million (ppm) relative to 4,4-dimethyl-4-silapentane-1-sulfonate as an internal reference.

Crystallization and Structure Determination. Crystals of F20H, F20M, F20Y, Y65A, and Y66L cyts c_3 were grown at 10 °C as reported.[4] For the crystallization, 2-methyl-2,4-pentanediol was used as the precipitant (an ethanol substitute). Diffraction experiments were carried out at 100 K using synchrotron X-ray beams (wavelength: 0.700 Å for F20H and Y65A, 1.000 Å for F20M and Y66L, and 0.710 Å for F20M cyts c_3) at SPring-8 (Table S1 in the Supporting Information). The crystals of all mutants belong to orthorhombic space group $P2_12_12_1$ except for that of Y66L cyt c_3, which belongs to $P2_1$. The diffraction data were processed and merged using the MOSFLM[11] and DCALA[12] programs, respectively. The structure refinement was performed with the CNS program[13] using the atomic coordinates of the wild-type cyt c_3 at 1.15 Å resolution[4] without water molecules, and followed by SHELXL.[14] All atoms including water oxygen were refined with anisotropic *B* factors. At the final stage of the refinement, hydrogen atoms were incorporated at the calculated positions. The root-mean-square deviation (RMSD) and accessible surface area (ASA) were calculated by means of the MolMol program.[15]

Results

Three-Dimensional Structures of Mutated Cytochromes c_3 in the Fully Oxidized State. The conserved noncoordinated aromatic residues, i.e., Phe20, Tyr43, Tyr65, and Tyr66 were shown to contribute to the extremely low reduction potentials of cyt c_3,[5–7] using amino acid replacements. To examine the effects of the mutations on the atomic structure, we have determined the crystal structures of fully oxidized F20H, F20M, F20Y, Y65A, and Y66L cyts c_3 at high resolution. The crystal structure of Y43L cyts c_3 was previously reported[5] (PDB ID 1J0P). The crystallographic data of these mutant proteins are listed in Table S1. Their atomic coordinates have been deposited in the Protein Data Bank (PDB) under Entries 2EWU (F20H), 2YYW (F20M), 2EWI (F20Y), 2YYX (Y65A), and 2Z47 (Y66L).

Since Phe20 is the most important residue, the structures around hemes 1 and 3 for F20H, F20M, and F20Y cyts c_3 are presented in Figure 2, and the structural parameters of the four hemes are summarized in Table 1. To our surprise, the conformational change induced by a mutation takes place only at the mutated residue in terms of the root-mean-square deviation (RMSD) and accessible surface area (ASA) for all

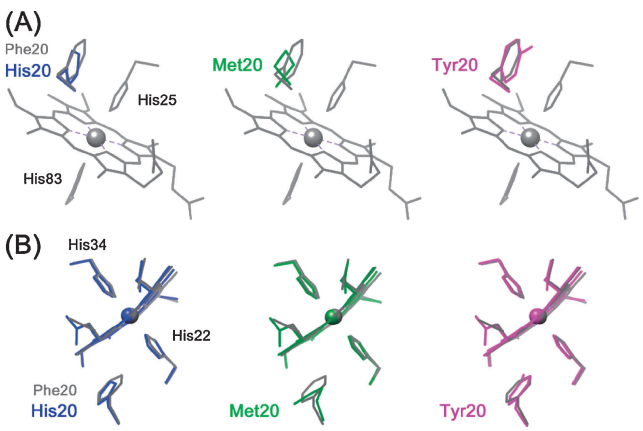

Figure 2. Crystal structures around hemes 3 (A) and 1 (B) of mutated cytochromes c_3. The two structures are superimposed in such a way that the porphyrins are best fitted. Grey, blue, green, and purple lines denote wild-type (PDB ID, 1J0O), F20H, F20M, and F20Y cytochromes c_3, respectively. The figures were prepared with UCSF Chimera.[3]

Table 1. Characterization of the Heme Structures on the Basis of X-ray Structures

	Wild type[a)]	F20H	F20M	F20Y	Y65A	Y66L
RMSD/Å[b),c)]						
Backbone		0.28	0.24	0.26	0.30	0.57
Heme 1		0.10	0.10	0.13	0.13	0.19
His34/His22		0.10/0.06	0.12/0.08	0.15/0.14	0.11/0.07	0.38/0.09
Heme 2		0.10	0.08	0.13	0.15	0.19
His52/His35		0.17/0.10	0.15/0.11	0.21/0.10	0.10/0.14	0.18/0.45
Heme 3		0.10	0.05	0.18	0.10	0.12
His83/His25		0.19/0.12	0.13/0.13	0.13/0.12	0.29/0.18	0.26/0.26
Heme 4		0.13	0.11	0.14	0.17	0.23
His106/His70		0.10/0.15	0.04/0.09	0.10/0.17	0.14/0.14	0.39/0.19
ASA[c)]/Å^2						
Heme 1	153.6	150.7	150.2	158.3	152.0	144.5
His34/His22[d)]	0.0/12.9	0.5/12.0	0.0/12.9	0.0/13.4	0.0/12.0	0.5/15.3
Heme 2	169.7	179.1	179.5	175.8	174.6	183.8
His52/His35[d)]	1.4/0.8	2.3/0.0	1.8/0.0	1.8/0.0	3.2/0.5	0.5/0.8
Heme 3	159.6	168.0	148.1	158.7	156.2	144.0
His83/His25[d)]	0.5/6.1	0.5/3.5	0.5/5.2	0.5/4.4	0.5/3.6	0.0/5.2
Heme 4	136.8	137.3	137.8	135.1	152.7	158.0
His106/His70[d)]	10.7/17.0	15.6/14.6	14.3/15.7	15.2/15.3	16.1/15.7	8.4/28.5
From Fe to $N_{\varepsilon 2}$[e)]/Å						
Heme 1–H34/H22	1.90/1.99	1.96/1.98	1.96/1.97	1.96/1.99	1.96/1.98	2.00/2.00
Heme 2–H52/H35	2.00/2.03	1.97/1.99	1.95/2.01	1.97/1.99	1.96/1.98	1.98/1.98
Heme 3–H83/H25	1.96/2.08	1.99/1.98	2.00/1.98	1.97/1.99	1.99/1.95	2.01/1.99
Heme 4–H106/H70	1.94/1.95	1.97/1.99	1.99/2.03	2.01/1.99	1.97/1.99	2.00/1.96
Angle of imidazoles[f)]/°						
Heme 1	4.3	4.0	0.5	4.0	3.0	2.5
Heme 2	69.0	77.4	76.4	74.7	71.1	72.2
Heme 3	4.9	3.0	0.7	6.5	7.6	1.4
Heme 4	4.9	2.6	3.0	1.6	4.5	6.8

a) From PDB Entry 1J0O. b) The values are between those of the wild type (PDB ID, 1J0O) and mutants. c) The RMSD and accessible surface area were calculated with the MolMol program.[15] d) His34, His52, His83, and His106, and His22, His35, His25, and His70 represent the fifth and sixth ligands of hemes 1–4, respectively. e) Distances from heme irons to $N_{\varepsilon 2}$ of coordinated histidines. f) Angle of two ligated imidazole planes.

crystal structures determined. The angle of two coordinated imidazole planes also exhibits subtle change. Therefore, it can be concluded that any effect on a distant heme induced by these mutations should not be attributed to propagation of the conformational change. Our results are in contrast to the crystal structure of F20L cyt c_3 from *Dv* Hildenborough,[16] in which a significant conformational change was induced by the F20L mutation.

Assignment and Characterization of C2 Proton Signals of Coordinated Histidines in the NMR Spectrum of Ferric Cyt c_3. The NMR signal of the C2 proton (C2H) of a coordinated imidazole was indicated as a sensitive monitor for the coordination structure.[17] Therefore, each C2H signal of the coordinated His of ferric *Dv*MF cyt c_3 was assigned on the basis of chemical shift perturbations induced by the mutations that caused little changes in the crystal structures and the NMR chemical shifts except for those at the mutated sites. The eight C2H signals are labeled Im1–Im8, from high to low frequency (Figure 3). Im6 was already assigned to His34 (fifth ligand of heme 1, h1-5 hereafter) in a previous study.[7] Heme numbering and all aromatic residues in the structure are presented in Figure 1.

Im7 and Im8 are significantly perturbed by the H25M (h3-6) mutation as can be seen in the spectrum of the [d_3-methyl]Met-labeled H25M cyt c_3 (Figure 3A). Since its crystal structure revealed that the conformational perturbation is localized only at the mutated site,[4] they can be ascribed to the ligands of heme 3. The disappearance of both signals confirms that the C2 proton is sensitive to the coordination structure at the iron. Since the aromatic ring of Phe20 is parallel to the imidazole of His25 (h3-6) as can be seen in Figure 2A, mutations at Phe20 also affected Im7 and Im8 (Figures 3B–3E). The perturbation at Im8 is greater than that at Im7 for F20Y and F20M cyts c_3 (Figures 3B and 3C). The fifth and sixth coordination structures at heme 3 are almost the same in the crystal structures (Table 1). Therefore, the closest one should be most significantly perturbed. Now, Im7 and Im8 can be assigned to His83 (h3-5) and His25 (h3-6), respectively. The spectrum of F20H (Figure 3D) supports this assignment. The doublet at the highest field should be due to the two different protonation structures of the replaced His imidazole, namely, those protonated at N1 and N4, respectively.

Im3 was also significantly perturbed in the spectra of all cyts c_3 mutated at Phe20. In the crystal structure,[5] Phe20 is close to

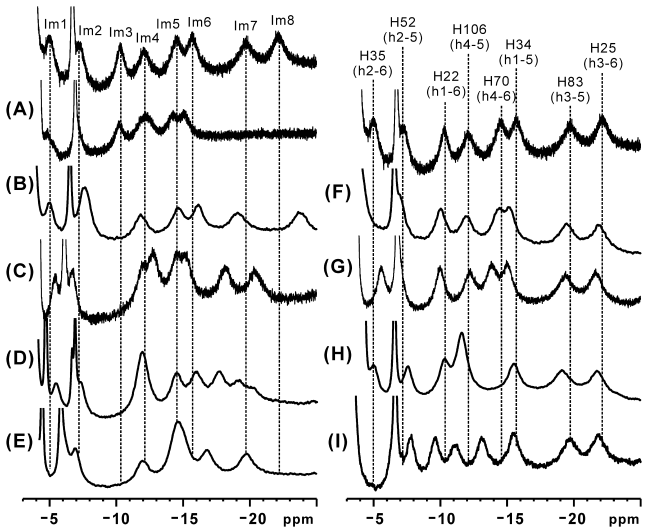

Figure 3. ^{1}H NMR spectra of C2 protons of the coordinated histidines in the ferric state for wild-type (Im1–Im8) and mutated *Dv*MF cytochromes c_3 at p^{2}H 7.0 and 303 K. Spectra for the wild-type are presented at the top of each column. (A) [d_3-methyl]Met-labeled H25M, (B) F20Y, (C) F20M, (D) F20H, (E) F20A, (F) F76Y, (G) H67Q, (H) Y66L, and (I) Y65A cytochromes c_3. The assignment of Im1–Im8 is shown at the top of the right column. Here, "hn-m" in parenthesis denotes the m-th ($m = 5$ or 6) ligand of heme n ($n = 1$–4).

His22 (h1-6) as well (Figure 2B). Although the angle of the imidazole planes at heme 2 changes by 6–8 degrees on mutation in the crystal structure (Table 1), the order in the extent of the angle change does not correlate with that in the chemical shift change of Im3. The changes in the chemical shifts of the other signals are minor. Thus, Im3 can be assigned to His22 (h1-6).

Im1 and Im5 are affected by the mutations of F76Y and Y66L, respectively (Figures 3F and 3H). Since the aromatic rings of Phe76 and Tyr66 are parallel to those of His35 (h2-6) and His70 (h4-6), Im1 and Im5 can be assigned to His35 (h2-6) and His70 (h4-6), respectively. The structures of F76Y and Y66L cyts c_3 were well characterized with NMR[6] and X-ray crystallography (Table 1), respectively, exhibiting the mutational perturbations only at the mutated sites.

Im2 and Im4 are left unassigned according to this method. For the assignment of these signals, we can use the information reported earlier. The temperature-dependence of the chemical shifts of the signals Im1–Im8 revealed that only Im1 and Im2 did not follow Curie's law.[17] Since this nonregular temperature-dependence must originate from the magnetic properties of a single coordinated iron, Im1 and Im2 should belong to the same heme, namely heme 2. Therefore, Im2 and Im4 can be assigned to His52 (h2-5) and His106 (h4-5), respectively. The assignment is presented on the top of Figure 3.

It was proposed on the basis of the analysis of high-spin cytochromes that the lower the resonance frequency of the C2H signal of the coordinated His is, the lower the reduction potential of the heme is.[18] The reduction potentials of hemes 1, 2, 3, and 4 of *Dv*MF cyt c_3 for the first reduction step ($e_1^{\rm I}$, $e_2^{\rm I}$, $e_3^{\rm I}$, and $e_4^{\rm I}$, respectively) are −309, −325, −285, and −252 mV, respectively.[6] The assignment mentioned above revealed that there is no direct correlation between the order of the reduction potentials of heme irons and that of the C2H chemical shifts (resonance frequencies) of the coordinated His residues. This is not consistent with the proposed relationship for high-spin cytochromes.[18] Both C2H signals of the sixth and fifth ligands of heme 3 (His25 and His83, respectively) shifted significantly on mutation, although only the signal of one ligand close to the mutated site was significantly affected in the case of the other hemes. This suggests that the trans effect in the chemical shift perturbation is most significant at heme 3. This also confirms that the π–π interaction between Phe20 and His25 (h3-6) actually induces a change in the electronic state of the π-orbital in the coordinated imidazole, which affects that in the other imidazole (His83 (h3-5)) through the iron.

Table 2. The Molecular Reduction Potentials of the Wild-Type and Mutated Cytochromes c_3 in 30 mM Sodium Phosphate Buffer (pH 7.0) at 30 °C[a),b),c)]

	$E_{\rm I}^{\rm o'}$/mV	$E_{\rm II}^{\rm o'}$/mV	$E_{\rm III}^{\rm o'}$/mV	$E_{\rm IV}^{\rm o'}$/mV	$E_{\rm ave}^{\rm o'}$/mV
Wild	−242	−296	−313	−358	−302
F20Y	−221	−256	−281	−334	−273 (+29)
F20M	−238	−269	−295	−343	−286 (+16)
F20H	−198	−239	−270	−315	−256 (+46)
F20A	−224	−255	−28	−314	−268 (+34)
Y65A	−227	−267	−296	−335	−281 (+21)
Y66L	−217	−288	−313	−358	−294 (+8)
H67Q	−243	−292	−315	−356	−302 (0)
F76Y	−234	−284	−313	−354	−296 (+6)

a) $E_i^{\rm o'}$ (i = I–IV) is the macroscopic reduction potential in the molecular level at the i-th reduction step relative to the standard hydrogen electrode (SHE). $E_{\rm ave}^{\rm o'}$ is the average of the four macroscopic reduction potentials. b) From Ref. 6. c) The standard errors are ± 2 mV.

To compare the effect of mutation on the C2H spectrum with that on the relative thermodynamic stabilities of the oxidation states, the molecular (or macroscopic) reduction potentials of *Dv*MF cyts c_3 used for the NMR experiments are summarized in Table 2.[6] They represent the reduction potentials of the whole protein at the four reduction steps, namely, one-, two-, three-, and four-electron reductions. The change in the average reduction potential is +16–+46 mV for the mutations at Phe20 and Tyr65, in contrast to that in 0–+8 mV for the other mutations. It reveals the important roles of Phe20 and Tyr65 in lowering of the reduction potentials. The spectral change in Figure 3 is also significant for the mutations at these residues, although only a single perturbation or slight perturbations were observed for the spectrum of the F70Y, Y66L, or H67Q cyt c_3 (Figure 3F, 3H, or 3G, respectively). In general, a more spectral change results in a greater change in the thermodynamic stability, suggesting an involvement of the coordination structures in the latter.

Discussion

The objective of this work is the elucidation of the mechanism underlying the stabilization of the oxidized heme irons of cyt c_3 by the π-electron systems, and the effect on the reduction potential of a distant heme induced by mutations at

Table 3. The Heme Reduction Potentials (mV) at the First Reduction Steps (e^{I}_i, Where i is the Heme Number) of the Wild-Type Cytochrome c_3, and the Differences in Those between the Mutant and Wild-Type Cytochromes c_3 (mV, from the Third to Ninth Rows)[a),b)]

	e_1^{I}	e_2^{I}	e_3^{I}	e_4^{I}
Wild-type	−309	−325	−285	−252
F20H-wild	+95	+26	+49	+10
F20Y-wild	+63	+20	−5	+13
F20M-wild	+31	+13	−21	+3
F20E-wild	+83	+37	+35	+24
Y43L-wild[c)]	+44	+24	+13	−2
Y43F-wild[c)]	+4	+2	−3	−2
Y65A-wild	+40	+17	+32	−1
Y66A-wild	−33	+13	−9	+32
Y66F-wild	−7	−6	−13	−3

a) e^{I}_i; the microscopic reduction potential of heme i at the first reduction step relative to the standard hydrogen electrode (SHE). b) The values are from Ref. 6. c) The values are from Ref. 5.

noncoordinated aromatic amino acids with a major emphasis on Phe20. To discuss these issues, the changes in the heme (or microscopic) reduction potentials (Δe_i^{I}; i, heme number; I, the first reduction step) are summarized in Table 3 for relevant cyt c_3 mutants.[6] Since we only have the crystal structures of the fully oxidized cyt c_3, we will discuss only the reduction potentials at the first reduction step. The crystal structures of Y43L cyt c_3[5] and those in Table 1 revealed that the conformational change in comparison with the structure of the wild-type cyt c_3 is localized to each mutation site. We assume that the subtle structural change induced by mutation also holds in the one-electron-reduced state. This is a reasonable assumption because of the following observation. The chemical shift of 7^1 CH_3 of heme 3 showed a nonlinear change only at the third reduction step.[19] Since this heme methyl group is located in the core of the heme architecture, the chemical shift is sensitive not only to the oxidation state, but also to the structure. The nonlinear change in the chemical shift should reflect a structural change in the protein. Therefore, no major structural change should take place at the first reduction step. On the basis of the assumption mentioned above, it can be concluded that the effects of the mutations in Table 1 and Y43L on the reduction potentials should be induced by physicochemical interactions without substantial conformational changes.

It was shown in our previous work that the replacement of an aromatic ring parallel to the coordinated imidazole with a nonaromatic side-chain causes the increase of the reduction potential of the local heme by about 40 mV (F20E, Y43L, and Y66A in Table 3) except for the mutation at F76, a non-conserved amino acid.[5,6] We ascribed increase of e^{I} to the loss of the apparent π–π interaction. In Figure 3, the chemical shift perturbation induced by the mutation at Phe20 was observed for both C2H signals of heme 3, Im7, and Im8. This confirmed that the π–π interaction between Phe20 and His25 (h3-6) actually affects the electronic state of the π-orbital in the His25 imidazole. The mechanism underlying the trans effect should be the π-back donation.

Phe20 is also parallel to the heme 1 (h-1) porphyrin. The F20M mutation increased e_1^{I} by 31 mV in spite of the π characteristics of Met exhibited in the interaction with His25 (h3-6).[6] Therefore, an aromatic ring at this site should be important for the stabilization of the oxidized h-1 iron. On the other hand, the F20Y mutation induced more increase (63 mV), even if Tyr has an aromatic ring similar to Phe. This is a unique property of the π–π interaction between the h-1 porphyrin and the Phe20 ring, in contrast to the π–π interactions at Tyr43 and Tyr66. In the latter case, the replacement of Tyr with Phe induced only small changes in the reduction potentials e_1^{I} and e_4^{I}, respectively, as can be seen in Table 3. This is also the case with the effect of the F20Y mutation on e_3^{I}. This indicates that the direct electrostatic interaction of the electric dipole in the Tyr ring with the oxidized iron is small. The effect of the F20Y mutation on e_1^{I} reveals that the electric dipole of the Tyr ring should destabilize the h-1 iron mainly through the interaction with the π-electrons of the porphyrin. The effect of the polarity was more significant for the F20H and F20E cyts c_3 (Table 3). Here, His and Glu are not ionized.[6] The increase in e_3^{I} induced by the F20H or F20E mutation can for the most part be explained by the loss of the π–π interaction. Consequently, His and Glu affect the reduction potential of the h-1 iron through the interaction with the π-electrons of the h-1 porphyrin as in the case of Tyr. The significant effect of the polar group indicates that the iron-induced polarization of the π-electron density in the porphyrin plays a role in lowering the reduction potential. This is different from the coordination interaction. Phe20 must stabilize the electrostatic interaction of the polarized π-electron density of the h-1 porphyrin with the oxidized iron through the π–π interaction. The electrostatic perturbation induced by the oxidized iron can be stabilized adaptively and efficiently by the change in the π-electron density distribution in the Phe20 ring, because there is no permanent dipole. The adaptive ability of the nonpolar aromatic ring would play an important role in the environmental change such as in the reduction/oxidation reaction. In conclusion, there are two kinds of π–π interactions that can contribute to lowering of the reduction potentials of cyt c_3. One involves the axial imidazole, and the other the porphyrin. The latter is a new mechanism found in this work.

As can be seen in Table 3, the increase in the reduction potential of a distant heme in the first reduction step was also observed for hemes 2 and 4 on the F20H, F20Y, and F20M mutations. The iron–iron distances from heme 1 are 12.2 and 17.8 Å for hemes 2 and 4, respectively.[5] The change of about 20 mV should be great enough for discussion. The change was caused with the polar group introduced into the Phe20 site. Since the direct effects of the polar groups turned out to be small, the electrostatic perturbation on the π-electron density of the h-1 porphyrin induced by the polar group should affect the stability of at least the oxidized h-2 iron without significant conformational changes. Namely, a through-space interaction is working between the h-1 π-electron system and heme 2. Since the increase in e_2^{I} is greater for the replacement with the polar group than for that with Met at the Phe20 site, the nature of the through-space interaction should be electrostatic. The effect of the F20E mutation on e_2^{I} is also consistent with this idea. Thus, we can conclude that the h-2 iron interacts electrostatically with

the π-electrons of the h-1 porphyrin in the hydrophobic core of cyt c_3. It is similar to the cation–π interaction, which was originally reported for compact metal–organic compounds[20a,20b,21,22] and then found to be important also in proteins and protein complexes.[20,23,24] The oxidized iron will be stabilized through the interaction with the original electron density, the induced dipole and the quadrupole in the π-electron system of the porphyrin.[20,21] It should work as one of factors stabilizing the oxidized h-2 iron, which is also a new mechanism contributing to regulation of the reduction potentials in cyt c_3. Although we can evaluate the change induced by the mutation, we cannot determine the quantitative contribution of its interaction in the wild-type cyt c_3 at this stage.

In general, these kinds of interactions will take place not only for the pair of hemes 1 and 2 but also for the other pairs of the hemes, leading to multiple interheme interactions in the tetraheme-architecture. Actually, a previous observation suggested at least the involvement of heme 2 in this kind of interaction. In the expression of H52M *Dv*MF cyt c_3, heme 2 was not incorporated into the protein because of the mutation at the fifth ligand.[4] Thus, there are only hemes 1, 3, and 4 in this protein. The midpoint potential of this triheme cyt c_3 was higher than that of the wild type by about 50 mV. Since the reduction potentials of heme 2 at the first and the fourth reduction steps, and the midpoint potential of the wild-type cyt c_3 are -325, -315, and -302 mV, respectively, simple elimination of heme 2 cannot explain the increase in the midpoint potential by about 50 mV. Therefore, the loss of heme–heme interactions should also contribute to this increase.

Conclusion

In conclusion, we have successfully identified three of the physicochemical interactions without substantial conformational changes indicated above. They are the π–π interaction between the axial imidazole and a noncoordinated aromatic ring, the π–π interaction between the porphyrin and a phenylalanine, and the electrostatic interaction between the porphyrin and a distant oxidized iron. The involvement of the π-electrons of the porphyrin in the electrostatic interaction stabilizing an oxidized heme iron has not been reported for cyt c_3 as summarized in the introduction. This kind of interaction provides new insight into the role of the heme architecture in regulation of the reduction potentials. Furthermore, these interactions involve Phe20, which is a key device not only to build up the compact configuration of hemes 1 and 3, but also to reduce their reduction potentials. For the first time, this work provided a rationale for the almost complete conservation of Phe20 in cyt c_3. It should be noted that the π–π interaction is also reported to stabilize the cation–π interaction. Reddy et al. found many cation–π–π structural motifs in PDB and CSD databases and their energy calculation exhibited the parallel stacking of aromatic rings being most efficient.[25] This result is consistent with the role of Phe20 in cyt c_3.

We thank Dr. Yoshitsugu Shiro of the RIKEN SPring-8 Center for the helpful discussion. This research was partly supported by a Grant-in-Aid for Scientific Research on Priority Areas from the Ministry of Education, Culture, Sports, Science and Technology of Japan to H.A., and by The National Project on Protein Structural and Functional Analyses, Japan, to Y.H. This was also supported by a WCU Grant from Korean Research Foundation funded by the Korea government, MEST to H.A.

Supporting Information

The crystallographic data are available free of charge on the Web at http//www.csj.jp/journals/bcsj/.

References

1 M. V. Pattarkine, J. J. Tanner, C. A. Bottoms, Y.-H. Lee, J. D. Wall, *J. Mol. Biol.* **2006**, *358*, 1314.
2 H. Akutsu, Y. Takayama, *Acc. Chem. Res.* **2007**, *40*, 171.
3 E. F. Pettersen, T. D. Goddard, C. C. Huang, G. S. Couch, D. M. Greenblatt, E. C. Meng, T. E. Ferrin, *J. Comput. Chem.* **2004**, *25*, 1605.
4 Y. Takayama, N. D. Werbeck, H. Komori, K. Morita, K. Ozawa, Y. Higuchi, H. Akutsu, *Biochemistry* **2008**, *47*, 9405.
5 K. Ozawa, Y. Takayama, F. Yasukawa, T. Ohmura, M. A. Cusanovich, Y. Tomimoto, H. Ogata, Y. Higuchi, H. Akutsu, *Biophys. J.* **2003**, *85*, 3367.
6 Y. Takayama, E. Harada, R. Kobayashi, K. Ozawa, H. Akutsu, *Biochemistry* **2004**, *43*, 10859.
7 N. Yahata, T. Saitoh, Y. Takayama, K. Ozawa, H. Ogata, Y. Higuchi, H. Akutsu, *Biochemistry* **2006**, *45*, 1653.
8 E. Stellwagen, *Nature* **1978**, *275*, 73.
9 E. Harada, J. Kumagai, K. Ozawa, S. Imabayashi, A. S. Tsapin, K. H. Nealson, T. E. Meyer, M. A. Cusanovich, H. Akutsu, *FEBS Lett.* **2002**, *532*, 333.
10 Y. Takayama, Y. Kobayashi, N. Yahata, T. Saitoh, H. Hori, T. Ikegami, H. Akutsu, *Biochemistry* **2006**, *45*, 3163.
11 A. G. W. Leslie, *MOSFILM, Vers. 5.41*, Oxford University Press, Oxford, UK, **1990**.
12 Collaborative Computational Project, Number 4, *Acta Crystallogr., Sect. D* **1994**, *50*, 760.
13 A. T. Brünger, P. D. Adams, G. M. Clore, W. L. DeLano, P. Gros, R. W. Grosse-Kunstleve, J.-S. Jiang, J. Kuszewski, M. Nilges, N. S. Pannu, R. J. Read, L. M. Rice, T. Simonson, G. L. Warren, *Acta Crystallogr., Sect. D* **1998**, *54*, 905.
14 G. M. Sheldrick, T. R. Schneider, *Methods Enzymol.* **1997**, *277*, 319.
15 R. Koradi, M. Billeter, K. Wüthrich, *J. Mol. Graphics* **1996**, *14*, 51.
16 A. Dolla, P. Arnoux, I. Protasevich, V. Lobachov, M. Brugna, M. T. Giudici-Orticoni, R. Haser, M. Czjzek, A. Makarov, M. Bruschi, *Biochemistry* **1999**, *38*, 33.
17 H. Akutsu, M. Hirasawa, *FEBS Lett.* **1992**, *308*, 264.
18 L. Banci, I. Bertini, P. Turano, M. Tien, T. K. Kirk, *Proc. Natl. Acad. Sci. U.S.A.* **1991**, *88*, 6956.
19 T. Ohmura, T. Inobe, K. Kano, T. Horizumi, H. Akutsu, *J. Electroanal. Chem.* **1997**, *438*, 237.
20 a) D. A. Dougherty, *Science* **1996**, *271*, 163. b) J. C. Ma, D. A. Dougherty, *Chem. Rev.* **1997**, *97*, 1303.
21 D. Kim, S. Hu, P. Tarakeshwar, K. S. Kim, J. M. Lisy, *J. Phys. Chem. A* **2003**, *107*, 1228.
22 S. E. Wheeler, K. N. Houk, *J. Am. Chem. Soc.* **2009**, *131*, 3126.
23 J. P. Gallivan, D. A. Dougherty, *Proc. Natl. Acad. Sci. U.S.A.* **1999**, *96*, 9459.
24 P. B. Crowley, A. Golovin, *Proteins: Struct., Funct., Bioinf.* **2005**, *59*, 231.
25 A. S. Reddy, D. Vijay, G. M. Sastry, G. N. Sastry, *J. Phys. Chem. B* **2006**, *110*, 2479.